

Chelating Dialkoxide Titanium Complex: A Versatile Building Block for the Construction of Heterometallic Derivatives

Rosa Fandos,^{*[a]} Carolina Hernández,^[a] Antonio Otero,^{*[b]} Cesar Pastor,^[c] Pilar Terreros,^[d] Gabriel Aullón,^[e] and Santiago Álvarez^[e]

Abstract: The heterometallic complex $[\text{TiCp}^*(\text{O}_2\text{Bz})_2\text{AlMe}_2]$ (**2**) has been synthesised by reaction of $[\text{TiCp}^*(\text{O}_2\text{Bz})(\text{OBzOH})]$ (**1**) with AlMe_3 ($\text{Cp}^* = \eta^5\text{-C}_5\text{Me}_5$; Bz = benzyl). Complex **1** reacts with HOTf to yield the cationic derivative $[\text{TiCp}^*(\text{OBzOH})_2]\text{OTf}$ (**3**) ($\text{HOTf} = \text{HSO}_3\text{CF}_3$). Compound **3** reacts with $[\text{M}(\mu\text{-OH})(\text{cod})_2]$ ($\text{M} = \text{Rh, Ir}$; cod = cyclooctadiene) to render the early–late heterometallic complexes $[\text{TiCp}^*(\text{O}_2\text{Bz})_2\{\text{M}(\text{cod})_2\}]\text{OTf}$ ($\text{M} = \text{Rh}$ (**4**); Ir (**5**)). The molecular structure of complex **4** has been established by single-crystal X-ray diffraction studies.

Keywords: density functional calculations · heterometallic complexes · rhodium · titanium

Introduction

Alkoxide ligands are extensively used as ancillary groups in the synthesis of early transition metal complexes, since adequate substitution patterns allow for an important modification of the steric and electronic requirements of the metal centre.^[1]

Moreover, early transition metal alkoxide complexes are the subject of considerable attention on account of their fundamental role as precursors for homogeneous catalysts^[2,3] and their applications in the synthesis of glasses, ceramics and organic–inorganic materials.^[4] Besides, soluble metallic alkoxides can also serve as models for heterogeneous systems. Particularly, early transition metal alkoxides can be envisaged as models of heterogeneous catalyst supports^[5] and early–late heterometallic complexes can be used as models to provide insight into the chemistry at the interface between a metal and its oxide support.^[6]

On the other hand, chelating ligands are in the focus of much attention as framework ligands for Groups 4 and 5 metal centres, because they usually yield kinetically stable complexes.^[7,8]

In this field we have recently described the synthesis of the titanium alkoxide complex $[\text{TiCp}^*(\text{O}_2\text{Bz})(\text{OBzOH})]$ (**1**)^[9] and herein we report that it shows noteworthy features when compared to monoalkoxide or symmetric dialkoxide complexes: 1) it can behave as a Brønsted acid and therefore it can react with metal–alkyl complexes yielding the corresponding heterometallic complexes, and 2) the asymmetric dialkoxide moiety can behave as a Brønsted base and can be selectively protonated, while still remaining coordinated to the metal centre yielding a cationic versatile building block in molecular architectures construction.

[a] Dr. R. Fandos, Dr. C. Hernández
Departamento de Química Inorgánica, Orgánica y Bioquímica
Universidad de Castilla-La Mancha
Facultad de Ciencias del Medio Ambiente. Avda. Carlos III
s/n, 45071 Toledo (Spain)
Fax: (+34)925-268840
E-mail: rosa.fandos@uclm.es

[b] Prof. Dr. A. Otero
Departamento de Química Inorgánica, Orgánica y Bioquímica
Universidad de Castilla-La Mancha, Facultad de Químicas
Campus de Ciudad Real, Avd. Camilo José Cela, 10
13071 Ciudad Real (Spain)
Fax: (+34)926-295318
E-mail: antonio.otero@uclm.es

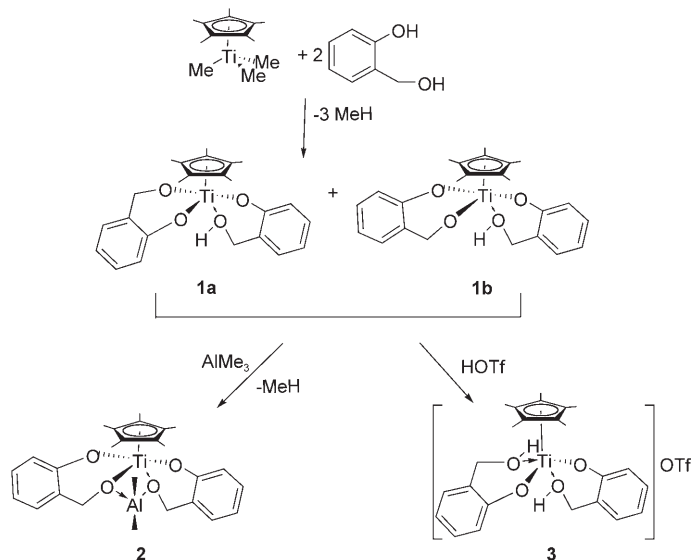
[c] C. Pastor
Servicio Interdepartamental de Apoyo a la Investigación
Facultad de Ciencias
Universidad Autónoma de Madrid (Spain)

[d] Dr. P. Terreros
Instituto de Catálisis y Petroleoquímica, CSIC
Cantoblanco, 28049 Madrid (Spain)

[e] Dr. G. Aullón, Prof. Dr. S. Álvarez
Departament de Química Inorgànica and
Centre de Recerca en Química Teòrica
Universitat de Barcelona, Diagonal 647
08028 Barcelona (Spain)

Results and Discussion

Complex **1** reacts with AlMe_3 to yield the heterometallic complex $[\text{TiCp}^*(\text{O}_2\text{Bz})_2\text{AlMe}_2]$ (**2**) (Scheme 1), which was isolated as a red crystalline solid. According to the spectro-

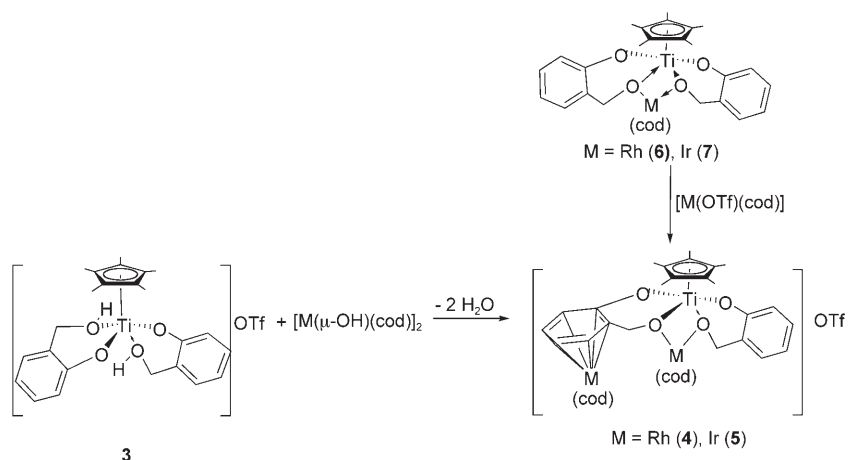


Scheme 1.

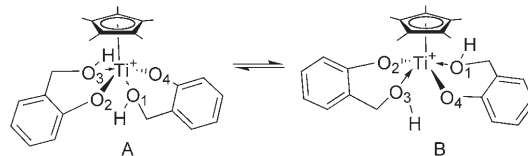
scopic and analytical data we propose complex **2** to be a heterometallic compound with the aluminium atom bonded to two methyl groups and to the methoxide moiety of both di-alkoxide ligands. The ^1H and ^{13}C NMR spectra of **2** fully agree with the proposed structure. The ^1H NMR spectrum shows two singlet signals at $\delta = -1.19$ and -0.42 ppm with an integral of 3H each; they are assigned to the methyl groups bonded to the aluminium atom. On the other hand, the spectrum shows a singlet at $\delta = 1.95$ ppm with a relative integral of 15H due to the protons of the Cp^* ligand on the titanium centre. The methylene protons of the alkoxide group give rise to two doublet signals at $\delta = 4.20$ and 4.60 ppm and the aromatic protons appear as multiplet absorptions at $\delta = 6.54$, 6.72 and 6.96 ppm.

Complex **1** can be protonated in a selective way with HOTf to yield the cationic derivative $[\text{TiCp}^*(\text{OBzOH})_2]\text{OTf}$ (**3**) (Scheme 1), which was isolated as an orange solid. The ^1H NMR spectrum of **3** in CD_2Cl_2 at room temperature indicates that both alkoxide ligands are in an equivalent chemical environment. On the other hand, the broadness of the methylene signal points to a slow rotation around the Ti–O

Scheme 3.



bond, probably because it is hindered by the additional coordination of the oxygen atom from the OH group to the metal centre. A ^1H variable temperature (VT) NMR measurement was carried out in CD_2Cl_2 in order to clarify this point. It shows that at 233 K the interchange between forms A and B (Scheme 2) is slow in the NMR timescale and,



Scheme 2.

therefore, the ^1H NMR spectrum is fully resolved. It shows that both methylene groups are in the same chemical environment, exhibit an AB pattern and appear as two doublet signals. The OH protons give rise to a doublet of doublets. Above 263 K, the signals, in the ^1H NMR spectrum, became broad and at 291 K (200 MHz) the methylene signals reach the coalescence.

Although the rapid exchange limit spectrum was not reached in the temperature range allowed by the solvent, these data point to the rapid interchange proposed in Scheme 2 that requires the opening of the Ti–OH bond.

Complex **3** reacts with $[\text{M}(\mu\text{-OH})(\text{cod})_2]$ ($\text{M} = \text{Rh}, \text{Ir}$) through a condensation reaction to yield the heterometallic cationic complexes $[\text{TiCp}^*(\text{O}_2\text{Bz})_2\text{M}(\text{cod})_2]\text{OTf}$ ($\text{M} = \text{Rh}$ (**4**); Ir (**5**)). Compounds **4** and **5** can be also prepared from the reaction of the previously reported^[9] complexes **6** or **7** and $[\text{M}(\text{OTf})(\text{cod})]$ (Scheme 3).

^1H and ^{13}C NMR spectroscopic data point to a quite asymmetric structure in both complexes, **4** and **5**; both methylene groups in the alkoxide ligands are different. An outstanding feature in both ^{13}C and ^1H NMR spectra is the chemical shift of the signals corresponding to the aromatic carbon and proton atoms, pointing to a quite different

chemical environment for the aromatic rings. To establish the molecular structure of these complexes a single-crystal X-ray diffraction study of **4** was carried out. The results confirmed the structural predictions based on analytical and spectroscopic data. Figure 1 shows an ORTEP diagram of **4**.

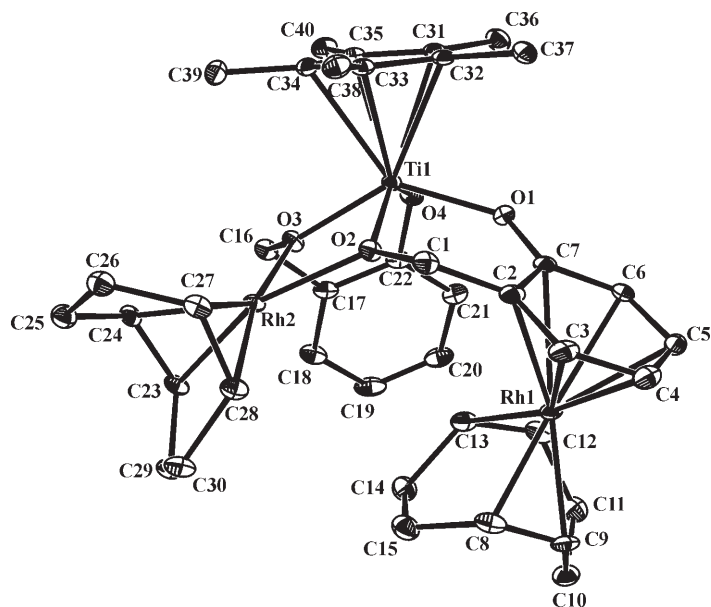


Figure 1. Structure of $[\text{TiCp}^*(\text{O}_2\text{Bz})_2[\text{Rh}(\text{cod})]_2]\text{OTf}$ (**4**). Selected bond lengths [Å] and angles [°]: Ti1–O4 1.913(2), Ti1–O1 1.962(2), Ti1–O3 1.974(2), Ti1–O2 2.020(2), Rh2–O2 2.092(1), Rh2–O3 2.062(2), Rh2–Ti1 3.2436(4), C2–C3 1.409(4), C2–C7 1.427(4), C3–C4 1.415(4), C4–C5 1.400(5), C5–C6 1.409(4), C6–C7 1.427(4), C7–O1 1.310(3), C17–C18 1.395(3), C18–C19 1.392(4), C19–C20 1.379(4), C20–C21 1.395(4), C21–C22 1.394(4), C22–O4 1.351(3); O3–Rh2–O2 72.38(6), O3–Ti1–O2 75.78(6), O4–Ti1–O1 86.75(7), C7–O1–Ti1 135.65(16), C22–O4–Ti1 124.28(14).

The structure is built up of discrete trimetallic (TiRh_2) molecules in which one of the rhodium centres is bonded to two oxygen atoms of the dialkoxide moiety and to the cod ligand, while the second one is π -bonded to one of the aryl groups and to cod. The remarkable features are discussed below. Ti1–O4 and Ti1–O1 distances are somewhat longer than those found in other titanium complexes with aryloxy ligands.^[10] On the other hand, Ti1–O3 and Ti1–O2 distances are longer, as expected for bridging alkoxide ligands.^[11] The intermetallic Rh2–Ti1 distance compares well with that found in compound **6**.^[9]

To analyze the preferences of the $\text{Rh}(\text{cod})$ moiety toward the three alternative coordination sites of the Ti starting complex, we have carried out a density functional study on the deprotonated mononuclear complex $[\text{TiCp}^*(\text{O}_2\text{Bz})_2]^-$ (**1**) and on dinuclear adducts $[\text{TiCp}^*(\text{O}_2\text{Bz})_2\text{Rh}(\text{cod})]$ (**6**) with the three coordination modes shown below (**6a–c**).

The three isomers appear to correspond to minima in the potential energy surface, with relative energies shown in Table 1. In all cases the orbital occupations are consistent with the formal oxidation states of Ti^{IV} and Rh^{I} . The most

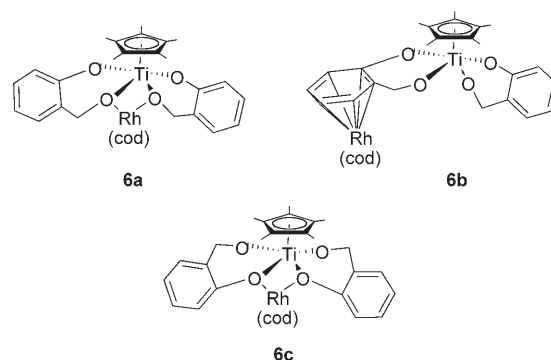


Table 1. Relative energies [kcal mol^{-1}] of the three isomers **6a–c** calculated in vacuo, in THF and in dichloromethane.

	6a	6b	6c
gas phase	0.0	21.8	25.3
THF	0.0	25.1	30.5
dichloromethane	0.0	25.6	29.3

stable coordination mode for Rh seems to be through the alkoxy groups, followed by π coordination from a benzo ring, while in the least stable isomer the Rh atom is coordinated by the phenoxo oxygen atoms.

The fact that the reaction of **1** with one mol of $\text{Rh}(\text{cod})$ leads to the alkoxy-bridged dinuclear complex (**6**)^[9] is in excellent agreement with the larger stability of coordination mode **6a**. Also the coordination of a second Rh^{I} center through the π system of a benzo ring is consistent with the stability order reflected in Table 1, in the gas phase, in THF and in dichloromethane. The lesser stability of the phenoxo-bonded isomer **6c**, relative to that of the alkoxy-bonded isomer **6a**, seems somewhat surprising at first sight. A closer analysis of their optimized structures (Figure 2) indicates that the coordination through the phenoxo groups has much higher steric hindrance associated to the different orientation of the oxygen lone pair that places the $\text{Rh}(\text{cod})$ moiety rather close to the Cp^* ring. Such destabilizing steric repulsion is reflected in a variety of structural parameters of **6c**: 1) one Me group of Cp^* (singled out in Figure 2) deviates significantly from the mean plane of the ring, 2) the Ti–O distance of the phenoxo groups in **6c** suffers a stronger elongation upon coordination to Rh (0.29 Å) than the corresponding distance of the alkoxy groups in **6a** (0.21 Å) and 3) the Rh–O distance is 0.06 Å longer when the coordination is through the phenoxo groups.

Even if the Rh–C bond lengths to the π -coordinated benzo ring are somewhat longer in the optimized structure **6b** than in the experimental trinuclear complex **4** (0.15 Å in average), similar structural features are found in both the optimized and the experimental structures. Thus, the benzo ring is seen to coordinate in an asymmetric way, suggesting an η^5 coordination compatible with the resonance form shown in Scheme 4, with some C=O double bond character, and consistent with the distribution of C–C, C=O and Rh–C

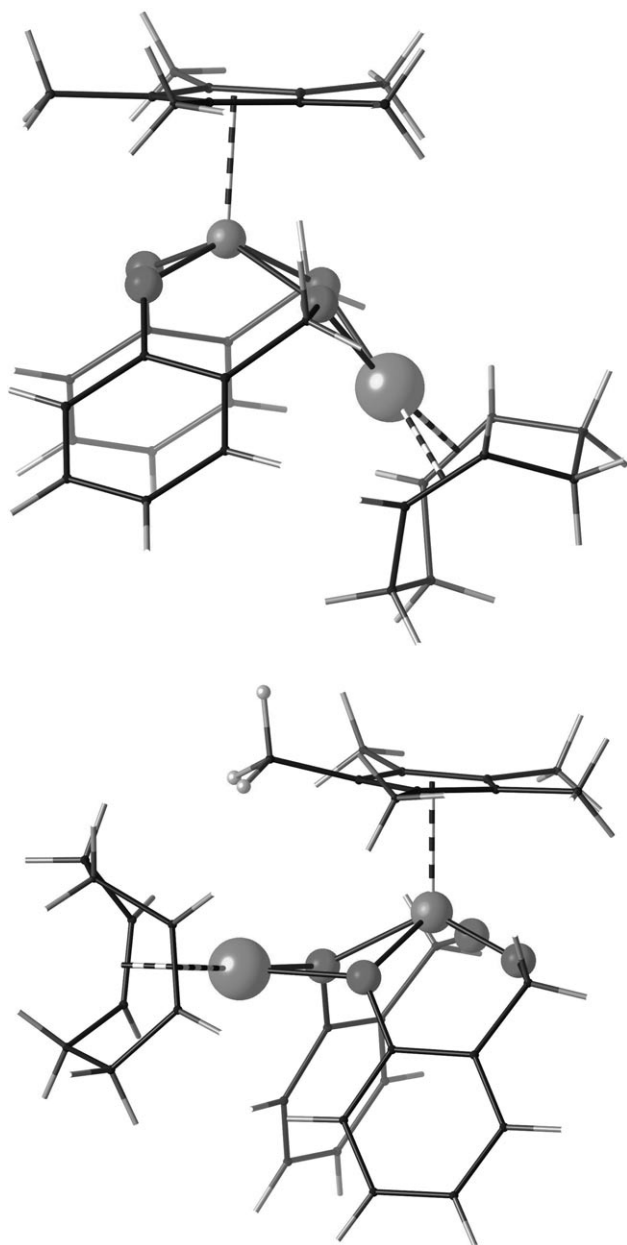
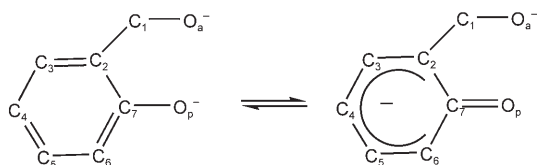


Figure 2. Optimized structures of isomers **6a** (top) and **6c** (bottom) of the dinuclear complex $[\text{TiCp}^*(\text{O}_2\text{Bz})_2\text{Rh}(\text{cod})]$, showing the different orientation and steric requirements of the $\text{Rh}(\text{cod})$ fragment in the latter case, as well as the significant deviation of one methyl group from the mean Cp plane.



Scheme 4.

bond lengths (Table 2). In contrast, the uncoordinated benzo ring presents quite similar C–C bond lengths as expected for a fully delocalized ring. Such a description, which

Table 2. Some bond lengths of the π -coordinated and non-coordinated benzo rings.

	coordinated		non-coordinated		
	exptl 4	calcd 6b	exptl 4	calcd 6b	calcd 1'
Rh–C7	2.386	2.642			
Rh–C2	2.373	2.499			
Rh–C3	2.291	2.388			
Rh–C4	2.265	2.292			
Rh–C5	2.297	2.444			
Rh–C6	2.293	2.567			
C7–O _p	1.310	1.272	1.351	1.340	1.326
C1–C2	1.508	1.513	1.497	1.514	1.511
C2–C3	1.409	1.398	1.395	1.397	1.393
C3–C4	1.415	1.423	1.392	1.396	1.400
C4–C5	1.400	1.426	1.379	1.397	1.398
C5–C6	1.409	1.391	1.395	1.394	1.394
C6–C7	1.429	1.449	1.393	1.410	1.411
C7–C2	1.426	1.457	1.413	1.413	1.418

suggests enhanced nucleophilicity of the coordinated benzo ring, is further supported by the different Ti–O distances presented by the Rh-coordinated and noncoordinated phenoxo groups: the coordinated group has Ti–O = 1.962 Å, whereas the noncoordinated one presents Ti–O = 1.913 Å, to be compared to the values shown by C=O–Ti and C–O–Ti groups found in the Cambridge Structural Database, of 2.08(7) and 1.86(9) Å.

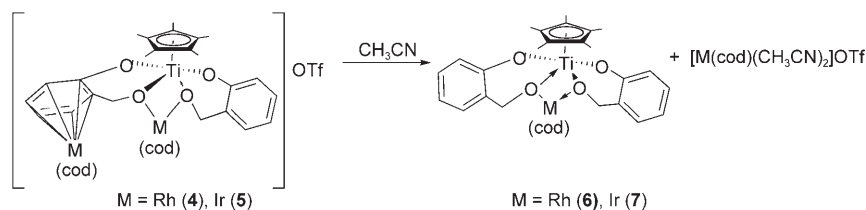
Further computational evidence for the importance of the η^5 resonant form of the benzo group comes from the calculated atomic charges (Table 3), by comparing those of the π -

Table 3. Calculated atomic charges of the optimized benzo groups and phenoxo oxygen atom, obtained from a natural population analysis.

Atom	π -coordinated		non π -coordinated		
	6b	6b	6a	6c	1'
O _p	–0.64	–0.69	–0.67	–0.72	–0.70
C7	+0.42	+0.34	+0.35	+0.36	+0.37
C2	–0.14	–0.13	–0.13	–0.12	–0.13
C3–C6	–1.11	–1.01	–1.00	–1.00	–1.05

coordinated ring in **6b** with the charges of the analogous uncoordinated ring in the same compound, in the other two isomers **6a** and **6c**, and with those in the mononuclear Ti complex **1'**. The phenoxo oxygen atom, for instance, is seen to lose more electron density upon π coordination through the carbon atoms in **6b** than when directly coordinated to Rh in **6c**. The C7 atom, on the other hand, has practically the same charge in all noncoordinated benzo rings, but becomes significantly more positively charged upon π coordination, whereas the negative charge on atoms C3 to C6 increases as expected for the η^5 resonant form.

In agreement with the reactivity expected for rhodium or iridium arene complexes,^[12] the π -coordinated benzo ring in complexes **4** and **5** can be easily displaced by acetonitrile to yield complexes **6** and **7** and the corresponding rhodium or iridium cationic derivatives (Scheme 5).



Scheme 5.

In summary, we have shown that the dialkoxide derivatives $[\text{TiCp}^*(\text{O}_2\text{Bz})(\text{OBzOH})]$ (**1**) and $[\text{TiCp}^*(\text{OBzOH})_2]\text{OTf}$ (**2**) are a versatile complexes for the construction of heterometallic derivatives, which have several available coordination positions. The preferences of the Rh(cod) moiety toward those coordination sites have been evaluated by means of a density functional study of the deprotonated mononuclear complex $[\text{TiCp}^*(\text{O}_2\text{Bz})_2]^-$ (**1'**) and the dinuclear adducts $[\text{TiCp}^*(\text{O}_2\text{Bz})_2\text{Rh}(\text{cod})]$ (**6**).

Experimental Section

General procedures: The preparation and handling of described compounds was performed with rigorous exclusion of air and moisture under nitrogen atmosphere using standard vacuum line and Schlenk techniques. All solvents were dried and distilled under a nitrogen atmosphere.

The following reagents were prepared by literature procedures: $[\text{TiCp}^*(\text{O}_2\text{Bz})(\text{O}_2\text{BzH})]$,^[9] $[\text{TiCp}^*(\text{O}_2\text{Bz})_2\text{M}(\text{cod})]$,^[9] $[\text{Rh}(\mu\text{-OH})(\text{cod})_2]$,^[13] $[\text{Ir}(\mu\text{-OH})(\text{cod})_2]$.^[14] The commercially available compounds like HOTf were used as received from Aldrich.

¹H and ¹³C NMR spectra were recorded on 200 Mercury Varian Fourier Transform spectrometer. Trace amounts of protonated solvents were used as references, and chemical shifts are reported in units of parts per million relative to SiMe₄.

Synthesis of $[\text{TiCp}^*(\text{O}_2\text{Bz})_2\text{AlMe}_2]$ (2**):** A solution of AlMe₃ in heptanes (0.59 mL, 1.18 mmol) was added to a solution of **1** (0.505 g, 1.18 mmol) in toluene (5 mL). The resulting solution was stirred at room temperature for 3 h and afterwards the solvent was removed under vacuum. The residue was extracted with pentane and the solution was cooled down to -25 °C for 48 h to yield red crystals of complex **2**. Yield: 0.238 g, 42%; ¹H NMR (200 MHz, C₆D₆): δ = -1.19 (s, 3H; AlMe), -0.42 (s, 3H; AlMe), 1.95 (s, 15H; Cp*), 4.20 (d, ²J(H,H) = 12.83 Hz, 2H; CH₂), 4.60 (d, ²J(H,H) = 12.83 Hz, 2H; CH₂), 6.54 (m, 2H; Ar), 6.72 (m, 4H; Ar), 6.96 ppm (m, 2H; Ar); ¹³C {¹H} NMR: δ = -11.0 (br, AlMe), -9.4 (br, AlMe), 12.0 (s, Cp*), 65.9 (s, O-CH₂), 117.0 (s, Ar), 119.3 (s, Ar), 125.3 (Cp*), 126.1 (s, Ar), 129.5 (s, Ar), 162.9 ppm (s, ipso); elemental analysis calcd (%) for C₂₆H₃₃AlO₄Ti: C 64.46, H 6.87; found: C 64.34, H 6.80.

Synthesis of $[\text{TiCp}^*(\text{OBzOH})_2]\text{OTf}$ (3**):** HOTf (0.068 mL, 0.77 mmol) was added to a solution of **1** (0.329 g, 0.77 mmol) in toluene (5 mL). The resulting solution was left to stand at room temperature for 14 h to allow the formation of a red solid that was separated by filtration and characterized as complex **3**. Yield: 0.283 g (64%); ¹H NMR (200 MHz, CD₂Cl₂, RT): δ = 2.13 (s, 15H; Cp*), 4.72 (br, 4H; OCH₂), 6.77 (m, 2H; Ar), 6.86 (m, 2H; Ar), 7.13 (m, 2H; Ar), 7.28 (m, 2H; Ar), 8.38 ppm (s, 2H; OH); ¹⁹F NMR: δ = -78.4 ppm (s, OTf); ¹³C {¹H} NMR: δ = 12.8 (s, Cp*), 66.9 (s, O-CH₂), 117.5 (s, Ar), 121.6 (s, Ar), 123.8 (Cp*), 127.6 (s, Ar), 130.9 (s, Ar), 133.9 (s, ipso Ar), 163.5 ppm (s, ipso); ¹H NMR (200 MHz, CD₂Cl₂, 233 K): δ = 2.08 (s, 15H; Cp*), 4.53 (dd, ²J(H,H) = 11.9 Hz, ³J(H,H) = 1.9 Hz, 2H; CH₂), 4.83 (dd, ²J(H,H) = 11.9 Hz, ³J(H,H) = 3.4 Hz, 2H; CH₂), 6.77 (m, 2H; Ar), 6.86 (m, 2H; Ar), 7.13 (m, 2H; Ar), 7.28 (m, 2H; Ar), 8.35 (dd, ³J(H,H) = 3.4 Hz, ²J(H,H) = 1.9 Hz, 2H; CH₂, OH); el-

emental analysis calcd (%) for C₂₅H₂₉F₃O₇STi: C 51.91, H 5.05; found: C 52.39, H 5.23.

Synthesis of $[\text{TiCp}^*(\text{O}_2\text{Bz})_2[\text{Rh}(\text{cod})_2]\text{OTf}$ (4**):** Dichloromethane (60 mL) was added to a mixture of complex **3** (0.143 g, 0.25 mmol) and $[\text{Rh}(\mu\text{-OH})(\text{cod})_2]$ (0.113 g, 0.25 mmol). The solution was stirred at room temperature for 1 h and then the solvent was removed under vacuum. The residue was washed

twice with Et₂O and identified as complex **4** (0.184 g, 74%). ¹H NMR (200 MHz, CDCl₃): δ = 1.87 (br, 8H; cod), 2.15 (m, 2H; cod), 2.21 (s, 15H; Cp*), 2.32 (m, 4H; cod), 2.60 (m, 2H; cod), 3.80 (m, 4H; cod, OCH₂), 4.00 (m, 1H; cod), 4.13 (m, 3H; cod), 4.34 (m, 2H; cod), 4.87 (m, 2H; OCH₂), 5.41 (m, 1H; Ar), 6.07 (m, 1H; Ar), 6.34 (m, 2H; Ar), 6.66 (m, 1H; Ar), 6.78 (m, 1H; Ar), 6.87 (m, 1H; Ar), 7.06 ppm (m, 1H; Ar); ¹⁹F NMR: δ = -79.2 ppm (s, OTf); ¹³C {¹H} NMR: δ = 13.1 (s, Cp*), 30.2 (s, cod), 30.5 (s, cod), 31.2 (s, cod), 31.8 (s, cod), 32.0 (s, cod), 32.7 (s, cod), 67.4 (s, O-CH₂), 69.9 (s, O-CH₂), 75.0 (d, ¹J(C,Rh) = 14.93 Hz, cod), 76.5 (d, ¹J(C,Rh) = 15.47 Hz, cod), 76.8 (d, ¹J(C,Rh) = 13.33 Hz, cod), 77.1 (d, ¹J(C,Rh) = 15.47 Hz, cod), 77.3 (d, ¹J(C,Rh) = 14.40 Hz, cod), 78.9 (d, ¹J(C,Rh) = 12.80 Hz, cod), 92.2 (s, Ar), 93.4 (d, ¹J(C,Rh) = 3.05 Hz, Ar), 100.6 (s, Ar), 105.9 (d, ¹J(C,Rh) = 3.06 Hz, Ar), 111.5 (s, Ar), 115.8 (s, Ar), 119.1 (s, Ar), 124.3 (s, Ar), 126.0 (s, Ar), 129.2 (s, Ar), 130.8 (Cp*), 151.2 (s, Ar), 164.1 ppm (s, Ar); elemental analysis calcd (%) for C₄₁H₅₁F₃O₇Rh₂Ti: C 49.31, H 5.15; found: C 49.28, H 5.37.

Synthesis of $[\text{TiCp}^*(\text{O}_2\text{Bz})_2[\text{Ir}(\text{cod})_2]\text{OTf}$ (5**):** Dichloromethane (60 mL) was added to a mixture of complex **3** (0.118 g, 0.20 mmol) and $[\text{Ir}(\mu\text{-OH})(\text{cod})_2]$ (0.127 g, 0.20 mmol). The solution was stirred at room temperature for 1 h and then the solvent was removed under vacuum. The residue was washed twice with Et₂O and identified as complex **5** (0.196 g, 81%). ¹H NMR (200 MHz, CD₂Cl₂): δ = 1.20–2.20 (m, 12H; cod), 2.31 (s, 15H; Cp*), 2.42 (m, 4H; cod), 3.43 (m, 1H; cod), 3.78 (m, 1H; cod), 4.00 (d, ²J(H,H) = 14.30 Hz, 1H; CH₂), 4.10 (m, 6H; cod), 4.37 (d, ²J(H,H) = 13.20 Hz, 1H; CH₂), 4.84 (d, ²J(H,H) = 14.30 Hz, 1H; CH₂), 5.11 (d, ²J(H,H) = 13.20 Hz, 1H; CH₂), 5.40 (m, 1H; Ar), 5.77 (m, 1H; Ar), 6.29 (m, 1H; Ar), 6.44 (m, 1H; Ar), 6.73 (m, 2H; Ar), 7.00 (m, 1H; Ar), 7.12 ppm (m, 1H; Ar); ¹³C {¹H} NMR: δ = 13.0 (s, Cp*), 30.8 (s, cod), 31.3 (s, cod), 31.8 (s, cod), 32.4 (s, cod), 32.9 (s, cod), 34.7 (s, cod), 57.3.2 (s, cod), 57.4 (s, cod), 58.8 (s, Hz, cod), 59.0 (s, cod), 61.9 (s, cod), 64.2 (s, cod), 67.6 (s, O-CH₂), 70.8 (s, O-CH₂), 82.4 (s, Ar), 91.3 (s, Ar), 94.2 (s, Ar), 98.6 (s, Ar), 101.9 (s, Ar), 116.3 (s, Ar), 120.2 (s, Ar), 124.6 (s, Ar), 126.7 (s, Ar), 129.9 (s, Ar), 132.4 (Cp*), 151.1 (s, Ar), 164.2 ppm (s, Ar); elemental analysis calcd (%) for C₄₁H₅₁F₃O₇Ir₂Ti: C 41.83, H 4.37; found: C 41.48, H 4.42.

Computational methods: Density functional calculations were carried out by using the GAUSSIAN98 package.^[15a] The hybrid density functional B3LYP method was applied.^[15b,c] Effective core potentials (ECP) and their associated double-ζ basis set, LANL2DZ, were used for transition metals (Ti and Rh).^[15d] A split-valence basis set with polarization functions, 6-31G*, was used for the main group light elements (C, H and O).^[15e,f] Geometry optimizations were carried out on the full potential-energy surface, without symmetry restrictions. Solvent effects were taken into account through the PCM algorithm,^[15g,h] using standard options of PCM and cavity keywords,^[15a] by calculating the energies with tetrahydrofuran and dichloromethane (ε = 7.58 and 8.93, respectively) as a solvent at the geometries optimized for the gas phase (single-point calculations).

X-ray crystallography: A suitable red crystal of compound **4** of approximate dimensions 0.25 × 0.10 × 0.08 mm with prismatic shape was mounted on a glass fiber and transferred to a Bruker SMART 6 K CCD area-detector three-circle diffractometer with a rotating anode (Cu_{Kα} radiation, λ = 1.54178 Å) generator equipped with Goebel mirrors at settings of 50 kV and 100 mA. X-ray data were collected at 100 K, with a combination of six runs at different φ and 2θ angles, 3600 frames. The data were collected using 0.3° wide ω scans (2 s per frame at 2θ = 40° and 10 s per

frame at $2\theta=100^\circ$, crystal-to-detector distance of 4.0 cm. Crystallographic data: formula: $C_{41}H_{51}F_3O_2Rh_2STi$; $M_r=998.60$; $T=100(2)$ K; crystal system: monoclinic; space group: $P2_1/n$; $a=9.4934(2)$, $b=33.1274(9)$, $c=12.4706(4)$ Å, $\alpha=90^\circ$, $\beta=93.1840(10)^\circ$, $\gamma=90^\circ$, $V[\text{Å}^3]=3915.84(18)$, $Z=4$, $\rho_{\text{calc}}=1.694$ Mg m $^{-3}$, $\mu=9.481$ mm $^{-1}$; $F(000)=2032$; θ range for data collection: $2.67\text{--}68.67^\circ$; index ranges: $-11\leq h\leq 11$, $-40\leq k\leq 40$, $-13\leq l\leq 15$; reflections collected: 29727; independent reflections: 6976 [$R(\text{int})=0.0306$]; completeness to $\theta=68.67^\circ$: 96.4%; absorption correction: semi-empirical from equivalents; data/restraints/parameters: 6976/0/501; goodness-of-fit on $F^2=1.034$; final R indices [$I>2\sigma(I)$]: $R1=0.0257$, $wR2=0.0679$; R indices (all data): $R1=0.0279$, $wR2=0.0694$; largest difference peak and hole: 0.786 and -0.366 e Å $^{-3}$.

The substantial redundancy in data allows empirical absorption corrections (SADABS)^[16] to be applied using multiple measurements of symmetry-equivalent reflections. The software package SHELXTL^[17–19] version 6.10 was used for space group determination, structure solution and refinement. The structure was solved by direct methods (SHELXS-97)^[18] completed with difference Fourier syntheses, and refined with full-matrix least-squares using SHELXL-97^[19] minimizing $\omega(F_o^2 - F_c^2)^2$. All non-hydrogen atoms were refined with anisotropic displacement parameters. The hydrogen atom positions were calculated geometrically and were allowed to ride on their parent carbon atoms with fixed isotropic U . CCDC-604194 (4) contains the supplementary crystallographic data for this paper. These data can be obtained free of charge from The Cambridge Crystallographic Data Centre via www.ccdc.cam.ac.uk/data_request/cif.

Acknowledgements

This work was supported by the Dirección General de Investigación (MEC, Spain), projects BQU2002-04638-CO2-02, ENE2004-07345-CO3-01 and CTQ2005-08123-CO2-01/BQU.

- [1] a) I. P. Rothwell, *Acc. Chem. Res.* **1988**, *21*, 153; b) I. P. Rothwell, *Chem. Commun.* **1997**, 1331.
- [2] J. Okuda, S. Fokken, T. Kleinhenn, T. P. Spaniol, *Eur. J. Inorg. Chem.* **2000**, 1321.
- [3] a) S. J. Sturla, S. L. Buchwald, *Organometallics* **2002**, *21*, 739, and references therein. b) N. W. Eilerts, J. A. Heppert, M. L. Kennedy, F. Takusagawa, *Inorg. Chem.* **1994**, *33*, 4813.
- [4] a) C. J. Brinker, D. E. Clark, D. R. Ulrich, in *Ceramics Through Chemistry*, Elsevier, New York, **1984**; b) R. C. Mehrotra in *Chemistry, Spectroscopy and Applications of Sol-Gel Glasses*, (Eds.: R. Reisfeld, C. K. Jorgensen), Springer, Berlin, **1992**.
- [5] R. T. Toth, D. W. Stephan, *Can. J. Chem.* **1991**, *69*, 172.
- [6] a) R. Fandos, C. Hernández, A. Otero, A. Rodríguez, M. J. Ruiz, P. Terreros, *Organometallics* **1999**, *18*, 2718; b) R. Fandos, J. L. Fierro, M. M. Kubicki, A. Otero, P. Terreros, M. A. Vivar-Cerrato, *Organometallics* **1995**, *14*, 2162; c) D. Selent, P. Claus, J. Pickardt, *J. Organomet. Chem.* **1994**, *468*, 131; d) M. S. Rau, C. M. Kretz, G. L. Geoffroy, A. L. Rheingold, B. S. Haggerty, *Organometallics* **1994**, *13*, 1624, and references therein. e) R. Xi, B. Wang, M. Abe, Y. Ozawa, K. Isobe, *Chem. Lett.* **1994**, 1177; f) R. Xi, B. Wang, M. Abe, Y. Ozawa, K. Isobe, *Chem. Lett.* **1994**, 323; g) K. Isobe, A. Yagasaki, *Acc. Chem. Res.* **1993**, *26*, 524.
- [7] Selected references: a) E. Y. Tshuva, S. Groysman, I. Goldberg, M. Kol, *Organometallics* **2002**, *21*, 662; b) E. Y. Tshuva, I. Goldberg, M. Kol, *J. Am. Chem. Soc.* **2000**, *122*, 10706; c) A. van der Linden, C. J. Schaverien, N. Nejboom, C. Ganter, A. G. Orpen, *J. Am. Chem. Soc.* **1995**, *117*, 3008; d) E. B. Tjaden, D. C. Swenson, R. F. Jordan, J. L. Petersen, *Organometallics* **1995**, *14*, 371; e) S. Fokken, T. P. Spaniol, J. Okuda, F. G. Sernetz, R. Mülhaupt, *Organometallics* **1997**, *16*, 4240; f) P. Shao, R. A. L. Gendron, D. J. Berg, G. W. Bushnell, *Organometallics* **2000**, *19*, 509; g) H. Mack, M. S. Eisen, *J. Chem. Soc. Dalton Trans.* **1998**, 917.
- [8] a) A. A. Naiini, S. L. Ringrose, Y. Su, R. A. Jacobson, J. G. Verkade, *Inorg. Chem.* **1993**, *32*, 1290; b) W. Menge, J. G. Verkade, *Inorg. Chem.* **1991**, *30*, 4628; c) A. Naiini, W. M. P. B. Menge, J. G. Verkade, *Inorg. Chem.* **1991**, *30*, 5009.
- [9] R. Fandos, C. Hernández, A. Otero, A. Rodríguez, M. J. Ruiz, P. Terreros, *Chem. Eur. J.* **2003**, *9*, 671.
- [10] A. V. Firth, D. W. Stephan, *Inorg. Chem.* **1998**, *37*, 4732.
- [11] V. W. Day, T. A. Eberspacher, J. Hao, W. G. Klemperer, B. Zhong, *Inorg. Chem.* **1995**, *34*, 3549.
- [12] A. C. Sievert, E. L. Muetterties, *Inorg. Chem.* **1981**, *20*, 489.
- [13] a) R. Usón, L. A. Oro, J. A. Cabeza, *Inorg. Synth.* **1985**, *23*, 126; b) D. Selent, M. Ramm, *J. Organomet. Chem.* **1995**, *485*, 135.
- [14] L. M. Green, D. W. Meek, *Organometallics* **1989**, *8*, 659.
- [15] a) Gaussian 98 (Revision A.11), M. J. Frisch, G. W. Trucks, H. B. Schlegel, G. E. Scuseria, M. A. Robb, J. R. Cheeseman, V. G. Zakrzewski, J. A. Montgomery, R. E. Stratmann, J. C. Burant, S. Dapprich, J. M. Millam, A. D. Daniels, K. N. Kudin, M. C. Strain, O. Farkas, J. Tomasi, V. Barone, M. Cossi, R. Cammi, B. Mennucci, C. Pomelli, C. Adamo, S. Clifford, J. Ochterski, G. A. Petersson, P. Y. Ayala, Q. Cui, K. Morokuma, D. K. Malick, A. D. Rabuck, K. Raghavachari, J. B. Foresman, J. Cioslowski, J. V. Ortiz, B. B. Stefanov, G. Liu, A. Liashenko, P. Piskorz, I. Komaromi, R. Gomperts, R. L. Martin, D. J. Fox, T. Keith, M. A. Al-Laham, C. Y. Peng, A. Nanayakkara, C. Gonzalez, M. Challacombe, P. M. W. Gill, B. G. Johnson, W. Chen, M. W. Wong, J. L. Andres, M. Head-Gordon, E. S. Replogle, J. A. Pople, Gaussian, Inc., Pittsburgh, PA, **2001**; b) A. D. Becke, *J. Chem. Phys.* **1993**, *98*, 5648; c) C. Lee, W. Yang, R. G. Parr, *Phys. Rev. B* **1988**, *37*, 785; d) P. J. Hay, W. R. Wadt, *J. Chem. Phys.* **1985**, *82*, 299; e) P. C. Hariharan, J. A. Pople, *Theor. Chim. Acta* **1973**, *28*, 213; f) M. M. Francl, W. J. Pietro, W. J. Hehre, J. S. Binkley, M. S. Gordon, D. J. DeFrees, J. A. Pople, *J. Chem. Phys.* **1982**, *77*, 3654; g) J. Tomasi, M. Persico, *Chem. Rev.* **1994**, *94*, 2027; h) C. Amovilli, V. Barone, R. Cammi, E. Cancès, M. Cossi, B. Mennucci, C. S. Pomelli, J. Tomasi, *Adv. Quantum Chem.* **1998**, *32*, 227.
- [16] Sheldrick, G. M. SADABS version 2.03, a Program for Empirical Absorption Correction, Universität Göttingen, Göttingen, **1997–2001**.
- [17] Bruker AXS SHELXTL version 6.10, Structure Determination Package, Bruker AXS **2000**. Madison, WI.
- [18] SHELXS-97, Program for Structure Solution: G. M. Sheldrick, *Acta Crystallogr. Sect. A* **1990**, *46*, 467.
- [19] Sheldrick, G. M. SHELXL-97, Program for Crystal Structure Refinement, Universität Göttingen, Göttingen **1997**.

Received: October 18, 2006
Published online: December 15, 2006